Supporting Information:

Metal-Coordinated Porphyrin COFs Enable Efficient Visible-Light-Driven Photocatalytic NADH regeneration

Qing-Ru Zhao,[a,†] Kui Wang,[b,†] Xiaokai Gao,[a] Hsien-Yi Hsu,[*c] and Chunyan Tan[*a,b]

[a]Institute of Biopharmaceutical and Health Engineering, Tsinghua Shenzhen International Graduate School, Tsinghua University, Shenzhen 518055, P. R. China.

[b]Open FIESTA, Tsinghua Shenzhen International Graduate School, Tsinghua University, Shenzhen 518055, P. R. China

[c]Department of Materials Science and Engineering, City University of Hong Kong, Kowloon Tong, Hong Kong, China.

† These authors contributed equally to this work.

E-mail: tancy@sz.tsinghua.edu.cn, sam.hyhsu@cityu.edu.hk

Table of Contents

1 Experimental

1.1 Materials

All reagents were obtained from commercial suppliers and were used without further purification: tetrakis(4-aminophenyl)porphyrin (Shanghai BiDe, 98%), [2,2'-bipyridyl]-5,5'-dialdehyde (Shanghai BiDe, 97%), dichloro(pentamethylcyclopentadienyl)rhodium (III) dimer (Shanghai BiDe, 98%), zinc acetate (Macklin, 99.9%), 1,2-dichlorobenzene (J&K, 99%), n-butanol (J&K, 99%), acetic acid (Macklin, 99%), tetrahydrofuran (Titan, 99%), acetone (Xilong Scientific Co., Ltd, AR), trichloromethane (Xilong Scientific Co., Ltd, AR), methanol (Titan, AR), ether (Xilong Scientific Co., Ltd, AR) and HPLC grade N,N-dimethylformamide (Meryer).

1.2 Instrumentation

Powder X-ray diffraction (PXRD) patterns were measured on a Rigaku Smartlab 9KW ray diffractometer. Fourier-transform infrared (FTIR) spectra were acquired using a Thermo Scientific Nicolet iS10 spectrometer. UV-vis diffuse reflectance spectra (DRS) were measured on a Shimadzu UV-3600i Plus spectrophotometer with an integrating sphere attachment, calibrated against $BaSO_4$ as a 100% reflectance standard. Electron paramagnetic resonance (EPR) spectra were collected on an EPR spectrometer (Bruker ELEXSYS-II E500, Germany). Solid-state ^{13}C cross-polarization magic angle spinning (CP/MAS) NMR spectra were collected on a Bruker AVANCE NEO 400 WB spectrometer operating at 100.63 MHz with a 4 mm MAS probe. All ^{13}C CP MAS chemical shifts are referenced to the resonances of adamantane standard. Nitrogen sorption isotherms at 77 K were measured using The samples were degassed for 12 h at 100 ℃ under vacuum prior to measurement. Brunauer-Emmett-Teller (BET) surface areas were calculated from the adsorption branch in the relative pressure (P/P_0) range of 0.05-0.30, and pore size distributions were derived using quenched solid density functional theory (QSDFT) with a slit-pore model. BBZM-I 350 W Research Xenon Cold Light Source; 50 W LED Cold Light Source; Shimadzu UV-2600 Ultraviolet-Visible Spectrophotometer, etc.

1.3 Synthesis

Synthesis of Por-Bpy-COF1. Tetrakis(4-aminophenyl)porphyrin (169 mg, 0.25 mmol) and [2,2′-bipyridyl]-5,5′-dialdehyde (109 mg, 0.5 mmol) were combined in a Pyrex tube. The solids were sonicated in a 1:1 (v/v) mixture of 1,2-dichlorobenzene (DCB, 12 mL) and n-butanol (n-BuOH, 12 mL) for 10 min, followed by addition of 6 M aqueous acetic acid (0.6 mL). The mixture was sealed under vacuum and degassed via three freeze-pump-thaw cycles. Reaction proceeded at 120 °C for 72 h in a silicone oil bath with agitation. After cooling to room temperature, the precipitate was collected by centrifugation, washed sequentially with ethanol and dichloromethane (3× each), Soxhlet-extracted with tetrahydrofuran (THF) and acetone for 8 h, and vacuum-dried at 80 °C overnight to afford Por-bpy-COF as black powder (228 mg, 82% yield).

Synthesis of Por-RhBpy-COF2. Accurately weigh 190 mg (0.3 mmol) of dichloro(pentamethylcyclopentadienyl)rhodium(III) dimer and dissolve it in 2 mL of ice-cold methanol. Next, weigh out 142 mg (0.67 mmol) of 2,2'-bipyridine-5,5'-dicarboxaldehyde and dissolve it in 8 mL of ice-cold methanol. Once both solutions are fully dissolved, slowly add the methanol solution of 2,2'-bipyridine-5,5'-dicarboxaldehyde to the methanol solution of dichloropentamethylcyclopentadienyl rhodium(III) dimer under stirring at 300 rpm, and continue stirring until the reaction mixture is completely clear, ensuring complete reaction between the two. After the reaction is complete, a large amount of ice-cold ether is added to the solution as a poor solvent to promote the precipitation of the product. The precipitated solid product is collected by filtration and dried using a hot air gun, ultimately yielding the target product，dichloro(pentamethylcyclopentadienyl)rhodium(III) coordinated 2,2'-bipyridine-5,5'-dicarboxaldehyde Rh/bpy.

Tetrakis(4-aminophenyl)porphyrin (135 mg, 0.2 mmol) and the above complex RhBpy (208 mg, 0.4 mmol) were combined in a Pyrex tube. The solids were sonicated in a 1:1 (v/v) mixture of 1,2-dichlorobenzene (DCB, 10 mL) and n-butanol (n-BuOH, 10 mL) for 10 min, followed by addition of 6 M aqueous acetic acid (0.5 mL). The mixture was sealed under vacuum and degassed via three freeze-pump-thaw cycles. Reaction proceeded at 120 °C for 72 h in a silicone oil bath with agitation. After cooling to room temperature, the precipitate was collected by centrifugation, washed sequentially with ethanol and dichloromethane (3× each), Soxhlet-extracted with tetrahydrofuran (THF) and acetone for 8 h, and vacuum-dried at 80 °C overnight to afford Synthesis of Por-RhBpy-COF2 as brownish black powder (246 mg, 71.7% yield).

Synthesis of ZnPor-RhBpy-COF3. Weigh 200 mg of tetrakis(4-aminophenyl)porphyrin and 260 mg of zinc acetate dihydrate into a 200 mL single-neck spherical reaction flask and place a magnetic stir bar inside. Seal the flask opening with a rubber stopper, connect the glass stopper to a double-tube system, and open the stopper. Perform three cycles of vacuum-nitrogen purging to completely remove oxygen. Under nitrogen protection, add methanol (20 mL), chloroform (90 mL), and N, N-dimethylformamide (30 mL) sequentially to the reaction flask as a mixed solvent. Then place the reaction flask in an oil bath, heat to 80 °C, and stir at 500 rpm for 24 hours. After the reaction is complete, cool the reaction mixture to room temperature and transfer it to a separating funnel. Add an appropriate amount of water to the funnel for washing, shake thoroughly to mix evenly, and then allow it to settle and separate into layers. Collect the lower organic layer and repeat the washing and layering operations three times to ensure the purity of the product. Subsequently, perform vacuum filtration on the organic layer to collect the precipitated solid product. Finally, dry the collected solid product at 80°C to obtain the target monomer ZnPor.

ZnPor (148 mg, 0.2 mmol) and the above complex RhBpy (208 mg, 0.4 mmol) were combined in a Pyrex tube. The solids were sonicated in a 1:1 (v/v) mixture of 1,2-dichlorobenzene (DCB, 10 mL) and n-butanol (n-BuOH, 10 mL) for 10 min, followed by addition of 6 M aqueous acetic acid (0.5 mL). The mixture was sealed under vacuum and degassed via three freeze-pump-thaw cycles. Reaction proceeded at 120 °C for 72 h in a silicone oil bath with agitation. After cooling to room temperature, the precipitate was collected by centrifugation, washed sequentially with ethanol and dichloromethane (3× each), Soxhlet-extracted with tetrahydrofuran (THF) and acetone for 8 h, and vacuum-dried at 80 °C overnight to afford ZnPor-RhBpy-COF3 as greenish black powder (231 mg, 64.9% yield).

1.4 General Procedure for Plotting the NADH Detection Standard Curve

Prepare NADH and NAD$^+$ solutions at concentrations of 0.01, 0.02, 0.05, 0.1, and

0.2 mM using PBS as the solvent. Detect the ultraviolet-visible absorption spectra using a spectrophotometer. Plot a standard curve for NADH regeneration by comparing the differences in absorption at 340 nm between NADH and NAD^+ solutions.

1.5 Light Source Selection

Configure the following system in Pyrex tubes: NAD 1 mM, COF 4 mg/ml, TEOA 10%, with PBS buffer as the solvent. Under strictly anaerobic conditions, irradiate with xenon lamp and LED light sources respectively for 1 hour of photocatalysis. Measure the absorbance of the system solution at 340 nm and calculate the NADH photocatalytic efficiency based on the NADH standard curve. Compare the efficiencies of the xenon lamp and LED light sources to investigate their impact on NADH regeneration efficiency.

Simultaneously, use an illuminance meter to detect the emission spectra of different light sources, analyze the proportion of usable light intensity and spectrum, and compare them with sunlight to determine the optimal light source selection.

1.6 General Procedure for COFs-Mediated Photocatalytic NADH Regeneration

Configure the following system in Pyrex tubes: NAD 1 mM, COF 1 mg/ml, TEOA 10%, with PBS buffer as the solvent. Under strictly anaerobic conditions, irradiate with a xenon lamp and perform photocatalysis for 0.5 h, 1 h, 2 h, and 8 h. Measure the absorbance of the system solution at 340 nm and calculate the photocatalytic efficiency of NADH based on the NADH standard curve.

The photocatalytic performance of three COFs—Por-Bpy-COF1, Por-RhBpy-COF2, and ZnPor-RhBpy-COF3—for NADH regeneration was compared by employing each as a photocatalyst.

2 Supplementary results and figures

2.1 Characterization of three COFs

A. Pore size

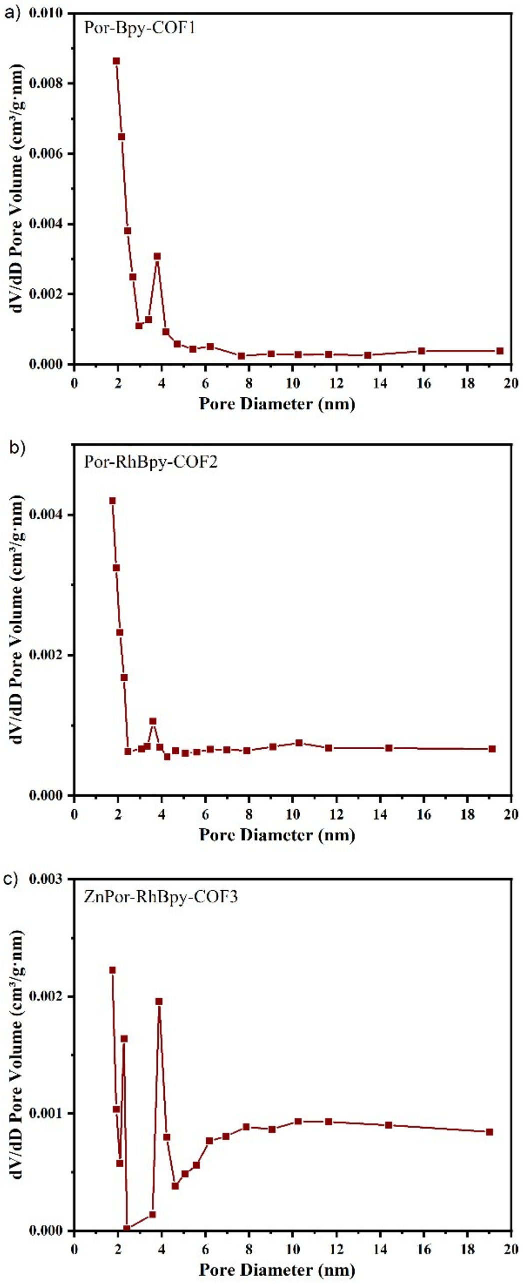

Figure S1 Pore size of Por-Bpy-COF1, Por-RhBpy-COF2, and ZnPor-RhBpy-COF3.

B. XPS

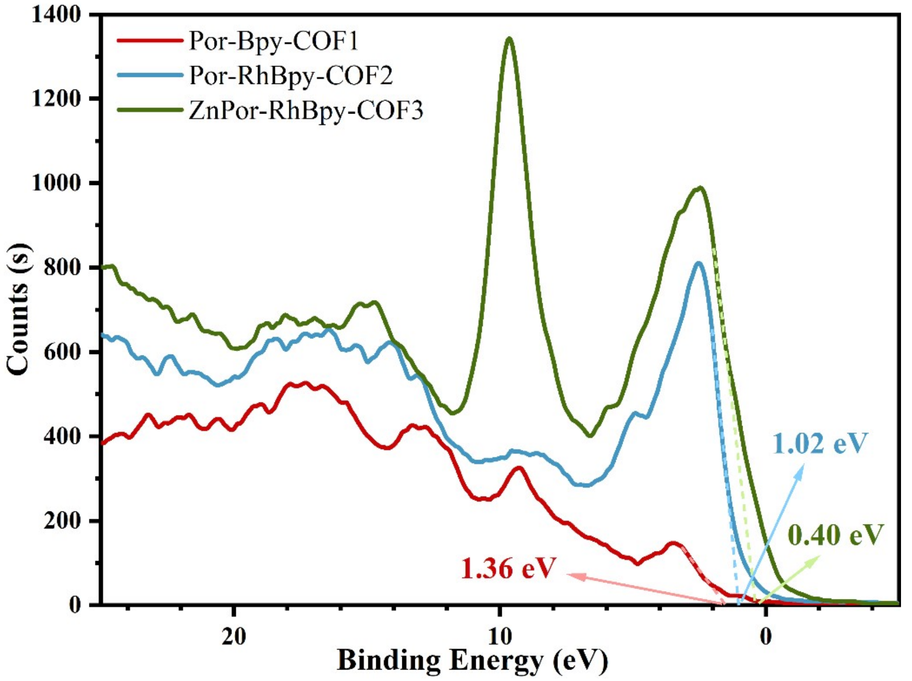

Figure S2 XPS spectra of Por-Bpy-COF1, Por-RhBpy-COF2, and ZnPor-RhBpy-COF3.

C. Photocurrent

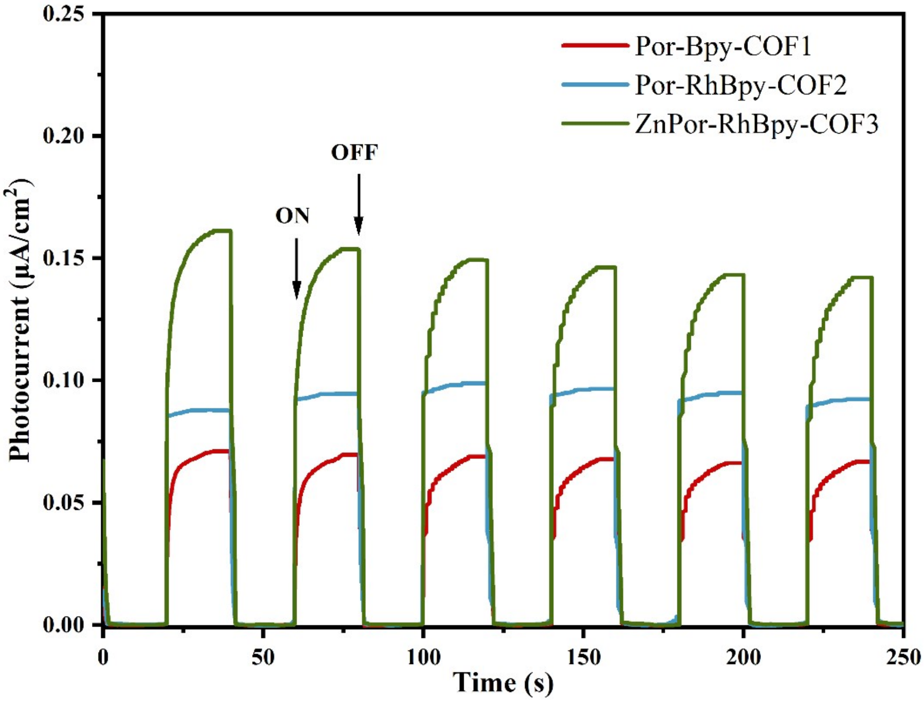

Figure S3 Photocurrent of Por-Bpy-COF1, Por-RhBpy-COF2, and ZnPor-RhBpy-COF3.

D. EIS

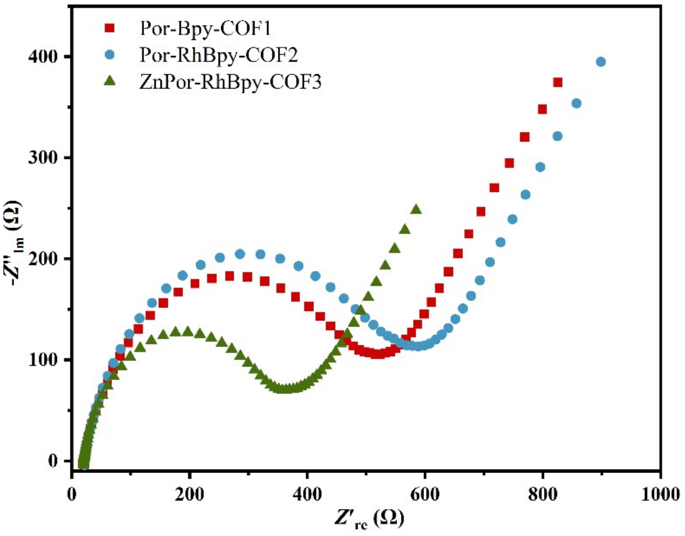

Figure S4 EIS of Por-Bpy-COF1, Por-RhBpy-COF2, and ZnPor-RhBpy-COF3.

2.2 COFs-Mediated Photocatalytic NADH Regeneration

A. Standard curve of NADH regeneration rate

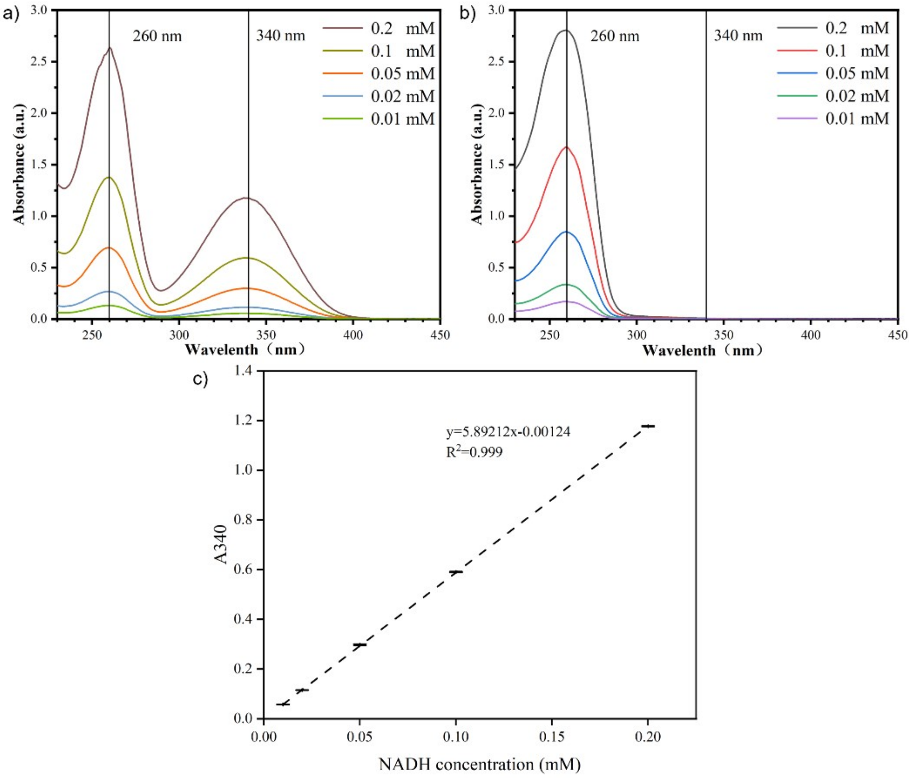

Figure S5 Standard curve of NADH regeneration concentration versus absorbance at 340 nm (a) Absorption spectra of NADH at different concentrations (b) Absorption spectra of NAD$^+$ at different concentrations (c) Standard curve of NADH regeneration rate.

B. NADH regeneration efficiency under different pH conditions

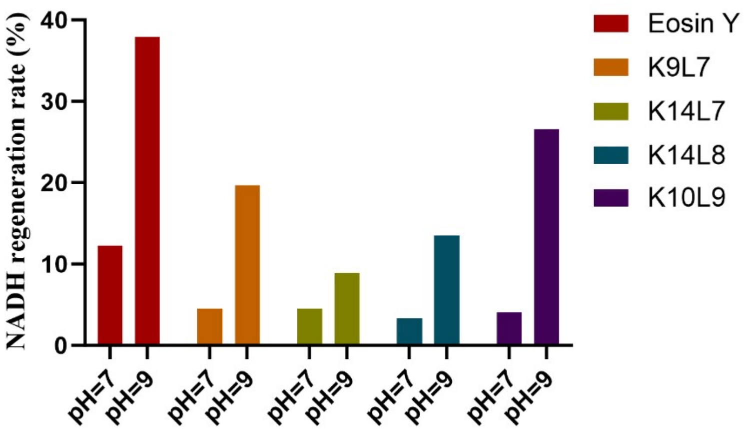

Figure S6 NADH regeneration efficiency under different pH conditions

C. Emission spectra under different light source conditions

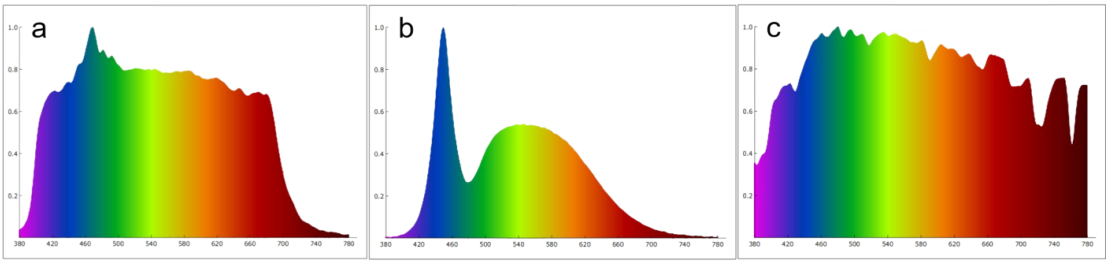

Figure S7 Emission spectra under different light source conditions. a) Xenon lamp, b) LED lamp, c) Sunlight.

D. Schematic diagrams of two non-porphyrin-based COFs

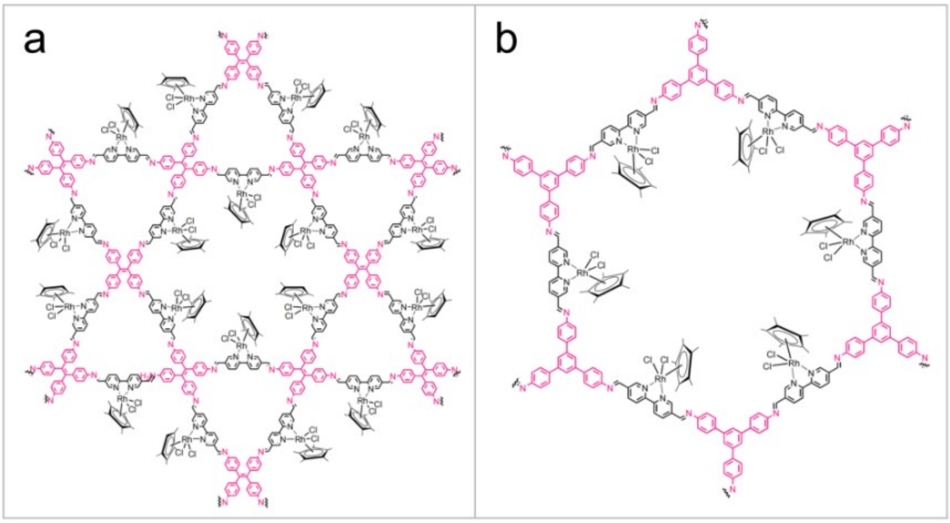

Figure S8 Schematic diagrams of two non-porphyrin-based COFs, a) ETTA-RhBpy-COF; b) TAPB-RhBpy-COF.

E. The Effect of Porphyrin Groups

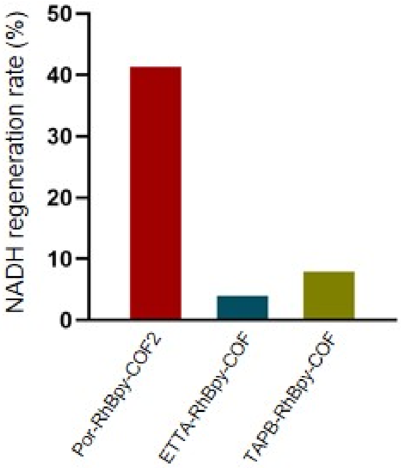

Figure S9 Photocatalytic NADH Regeneration Performance of Porphyrin-Based and Non-Porphyrin-Based COFs

F. NADH regeneration yield under different dosage conditions

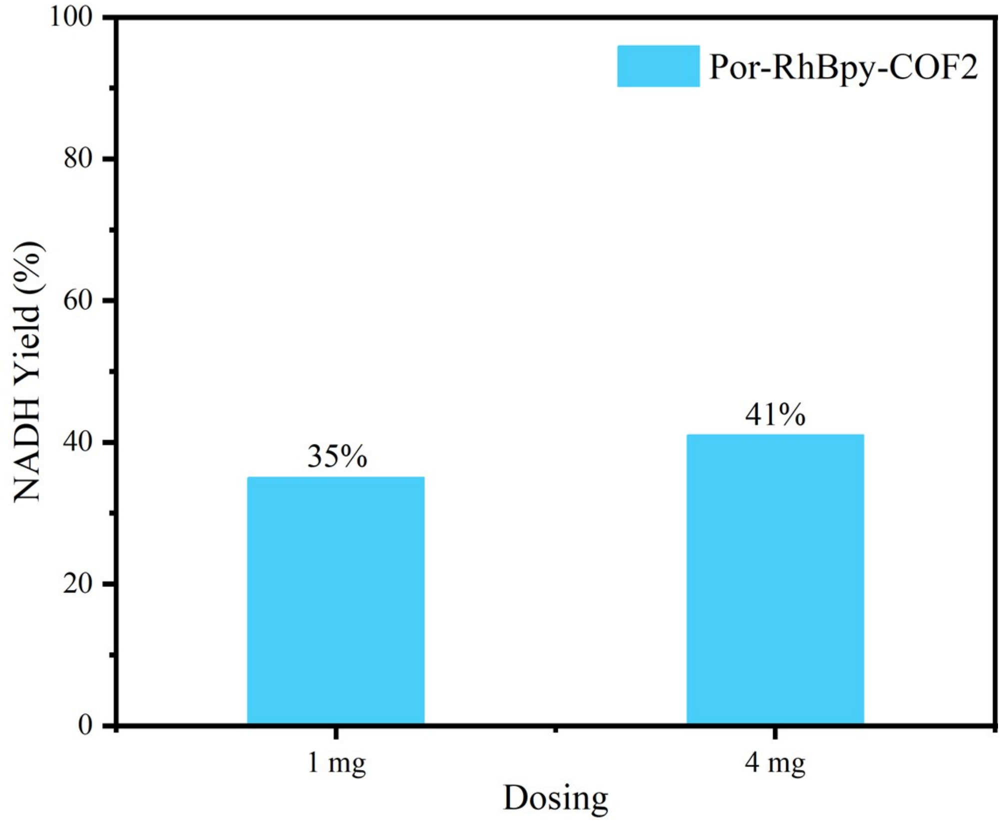

Figure S10 NADH regeneration yield under different dosage conditions

G. Solid-State NMR Characterization of Recycled Catalysts

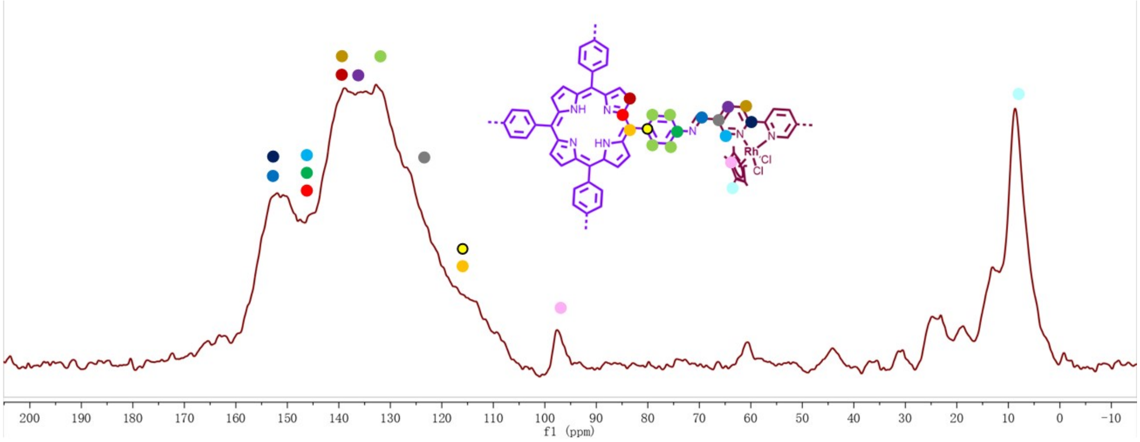

Figure S11 Solid-state NMR characterization of recycled catalysts.

H. FTIR of Recycled Catalysts

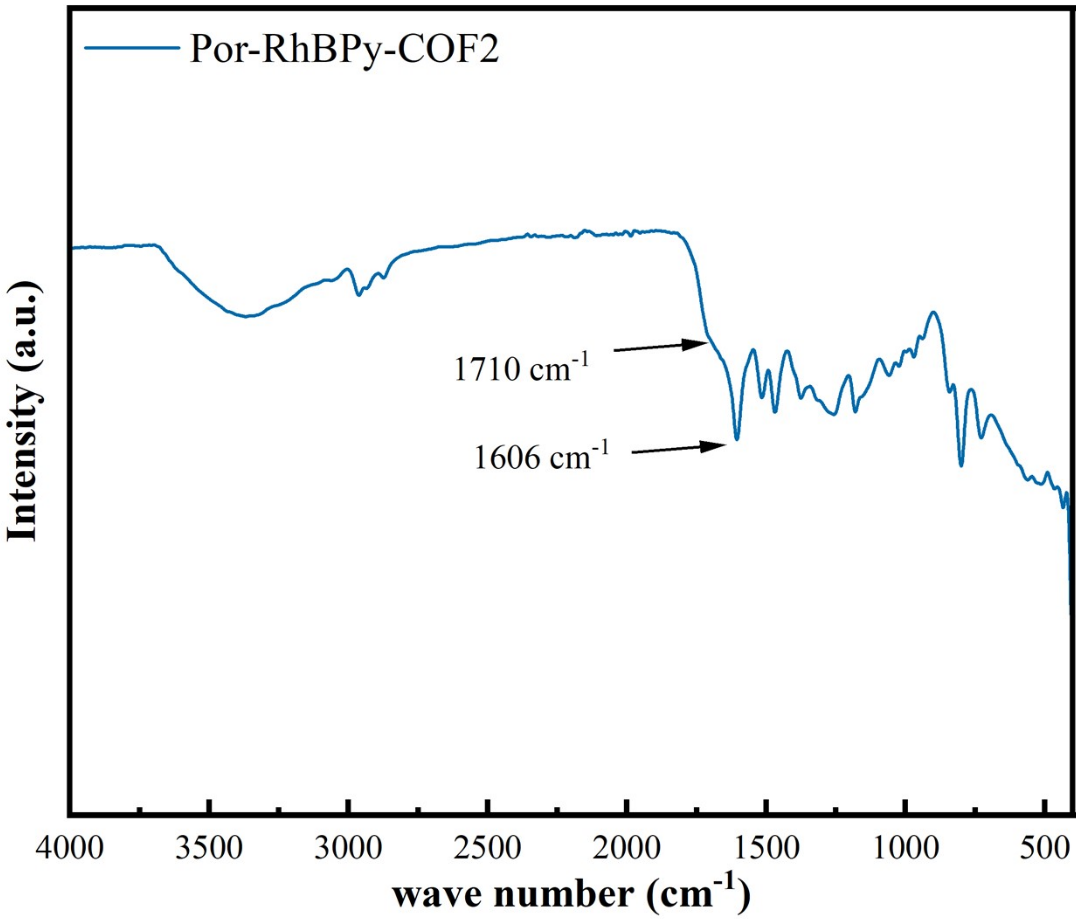

Figure S12 FTIR of recycled catalysts.